Inorg. Chem. **2006**, *45*, 8719–8728

Pyridine- and Phosphonate-Containing Ligands for Stable Ln Complexation. Extremely Fast Water Exchange on the Gd^{III} Chelates

Edina Balogh,[†] Marta Mato-Iglesias,[‡] Carlos Platas-Iglesias,*[,‡] Éva Tóth,*[,†,§] Kristina Djanashvili,[||] Joop A. Peters,[||] Andrés de Blas,[†] and Teresa Rodríguez-Blas[†]

Laboratoire de Chimie Inorganique et Bioinorganique, Ecole Polytechnique Fédérale de Lausanne, BCH, CH-1015 Lausanne, Switzerland, Departamento de Química Fundamental, Universidade da Coruña, Campus da Zapateira s/n, 15071 A Coruña, Spain, Biocatalysis and Organic Chemistry, Delft University of Technology, Julianalaan 136, 2628 BL Delft, The Netherlands, and Centre de Biophysique Moléculaire, CNRS, rue Charles Sadron, 45071 Orléans Cedex 2, France

Received March 10, 2006

Two novel ligands containing pyridine units and phosphonate pendant arms, with ethane-1,2-diamine (**L²**) or cyclohexane-1,2-diamine (**L³**) backbones, have been synthesized for Ln complexation. The hydration numbers obtained from luminescence lifetime measurements in aqueous solutions of the Eu^{III} and Tb^{III} complexes are $q =$ 0.6 (Eu**L²**), 0.7 (Tb**L²**), 0.8 (Eu**L³**), and 0.4 (Tb**L³**). To further assess the hydration equilibrium, we have performed a variable-temperature and -pressure UV–vis spectrophotometric study on the Eu^{III} complexes. The reaction enthalpy, entropy, and volume for the hydration equilibrium EuL $\leftrightarrow$ EuL(H_2O) were calculated to be $\Delta H^\circ = -(11.6 \pm 2)$ kJ mol^{-1}, $\Delta S^\circ = -(34.2 \pm 5)$ J mol^{-1} K^{-1}, and $K_{Eu}^{298} = 1.8 \pm 0.3$ for Eu**L²** and $\Delta H^\circ = -(13.5 \pm 1)$ kJ mol^{-1}, $\Delta S^\circ = -(41 \pm 4)$ J mol^{-1} K^{-1}, and $K_{Eu}^{298} = 1.7 \pm 0.3$ for Eu**L³**, respectively. We have carried out variable-temperature ^{17}O NMR and nuclear magnetic relaxation dispersion (NMRD) measurements on the Gd**L²**$(H_2O)_q$ and Gd**L³**$(H_2O)_q$ systems. Given the presence of phosphonate groups in the ligand backbone, a second-sphere relaxation mechanism has been included for the analysis of the longitudinal ^{17}O and ^1H NMR relaxation rates. The water exchange rate on Gd**L²**$(H_2O)_q$, $k_{ex}^{298} = (7.0 \pm 0.8) \times 10^8$ s^{-1}, is extremely high and comparable to that on the Gd^{III} aqua ion, while it is slightly reduced for Gd**L³**$(H_2O)_q$, $k_{ex}^{298} = (1.5 \pm 0.1) \times 10^8$ s^{-1}. This fast exchange can be rationalized in terms of a very flexible inner coordination sphere, which is slightly rigidified for **L³** by the introduction of the cyclohexyl group on the amine backbone. The water exchange proceeds via a dissociative interchange mechanism, evidenced by the positive activation volumes obtained from variable-pressure ^{17}O NMR for both Gd**L²**$(H_2O)_q$ and Gd**L³**$(H_2O)_q$ ($\Delta V^{\ddagger} = +8.3 \pm 1.0$ and 8.7 ± 1.0 cm^3 mol^{-1}, respectively).

Introduction

Stable chelates of trivalent Ln ions are gaining considerable interest because of their use in various biomedical applications, such as fluorescence imaging,[1] specific RNA cleavage,[2] cancer radiotherapy,[3,4] or magnetic resonance imaging (MRI).[5] The spectacular evolution of MRI into one of the most powerful modalities in clinical diagnostics has been indeed largely assisted by the development of Gd^{III}-based contrast agents.[6,7] Currently, about one-third of all MRI scans are made after the administration of a contrast agent,[7] which enhances the image contrast by preferentially influ-

* To whom correspondence should be addressed. E-mail: cplatas@udc.es (C.P.-I.), (E.T.).
[†] Ecole Polytechnique Fédérale de Lausanne, BCH.
[‡] Universidade da Coruña.
[§] CNRS.
[||] Delft University of Technology.

(1) *Bioanalytical Applications of Labeling Technologies*; Hemmilä, I., Stahlberg, T., Mottram, P., Eds.; Wallac Oy: Turku, Finland, 1994.
(2) Bruice, T. C.; Tsubouchi, A.; Dempey, R. O.; Olson, L. P. *J. Am. Chem. Soc.* **1996**, *118*, 9867.
(3) DeNardo, G. L.; Mirik, G. R.; Kroger, L. A.; O'Donnel, R. T.; Meares, C. F.; DeNardo, S. J. *J. Nucl. Med.* **1996**, *37*, 451.
(4) Heppeler, A.; Froidevaux, S.; Mäcke, H. R.; Jermann, E.; Béhé, M.; Powell, P.; Hennig, M. *Chem.—Eur. J.* **1999**, *5*, 1974.
(5) Lauffer, R. B. In *MRI Clinical Magnetic Resonance Imaging*, 2nd ed.; Edelman, R. R., Zlatkin, M. B., Hesselink, J. R., Eds.; W. B. Saunders Co.: Philadelphia, PA, 1996; Vol. 1, Chapter 5.
(6) *The Chemistry of Contrast Agents in Medical Magnetic Resonance Imaging*; Mebach, A. E., Tóth, É., Eds.; Wiley: New York, 2001.
(7) Caravan, P.; Ellinson, J. J.; McMurry, T. J.; Lauffer, R. B. *Chem. Rev.* **1999**, *99*, 2293.

10.1021/ic0604157 CCC: $33.50
Published on Web 09/12/2006

encing the relaxation rate of the water protons in the target tissue. The efficiency of a contrast agent is evaluated in terms of its relaxivity, which is defined as the paramagnetic relaxation rate enhancement of water protons per millimolar concentration of the Gd^{III} ion. These complexes contain at least one Gd^{III}-bound water molecule that exchanges with the bulk water of the body, resulting in an efficient mechanism for the longitudinal and transverse relaxation (T_1 and T_2) of water protons. The relaxation rates of the bulk water protons are enhanced around a paramagnetic ion because of long-range interactions (outer-sphere relaxation) and short-range interactions (inner-sphere relaxation). According to the standard Solomon−Bloembergen−Morgan model, the latter process is governed by four correlation times: the rotational correlation time of the complex (τ_R), the residence time of a water proton in the inner coordination sphere (τ_m), and the longitudinal and transverse electronic relaxation rates ($1/T_{1e}$ and $1/T_{2e}$) of the metal center.[8] The theory predicts that high relaxivities at the current imaging fields (0.5−1.5 T) may be observed for systems with a long rotational correlation time and relatively fast water exchange.

The modulation of the water exchange on Gd^{III} complexes has been the subject of extensive studies. The current commercial Gd^{III} chelates show water exchange rates that are 1 order of magnitude lower than the optimal value. Recently, it was shown that phosphonate-containing analogues of the commercially used $[Gd(DOTA)(H_2O)]^-$ and $[Gd(DTPA)(H_2O)]^{2-}$ complexes have faster water exchange than the parent systems.[9] A similar effect has also been observed for Gd^{III} complexes of heptadentate macrocyclic ligands.[10] These gadolinium(III) poly(aminocarboxylates) undergo a dissociative, D, or dissociative interchange, I_d, water exchange. Steric crowding around the bound water site is very important in such dissociative processes. Increased steric crowding facilitates the leaving of the bound water molecule in the rate-determining step, thus accelerating the water exchange. This phenomenon has been demonstrated for both acyclic and macrocyclic Gd^{III} complexes.[11,12] The presence of a bulky phosphonate group replacing a carboxylate in the framework of $DOTA^{4-}$ or $DTPA^{5-}$ also causes a crowding effect and a consequent increase in the water exchange rate of the Gd^{III} complex. However, the water exchange rate on these systems is still largely inferior to that of $[Gd(H_2O)_8]^{3+}$. The very high water exchange rate observed for $[Gd(H_2O)_8]^{3+}$ ($k_{ex}^{298} = 8.04 \times 10^8\ s^{-1}$)[13] as compared to

Chart 1

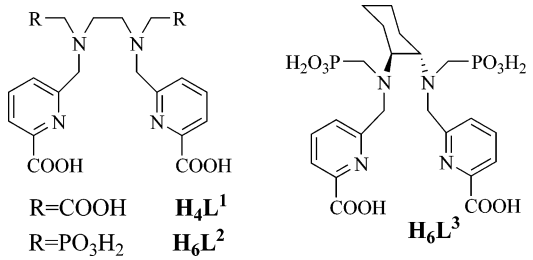

the usual gadolinium(III) poly(aminocarboxylates) can be related to the easy rearrangement of the flexible coordination sphere. The Gd^{III} aqua ion is eight-coordinate but very close to a hydration equilibrium between coordination numbers 8 and 9. Indeed, from neutron diffraction measurements, it is known that, as the ionic radius decreases in the Ln series, the coordination number of the aqua ions changes from 9 at the beginning to 8 at the end, with Sm^{III} having an average coordination number of 8.5.[14] In contrast, Gd^{III} chelates have a much more rigid inner-sphere structure and its rearrangement requires higher energy. On the basis of these considerations, faster water exchange is expected for Gd^{III} complexes with a hydration equilibrium, especially when they possess a flexible inner-sphere structure. In a preliminary paper, we have illustrated this approach to obtain fast water exchange rates in Gd^{III} complexes.[15]

In a recent work,[16] we reported a new octadentate receptor containing pyridine units and carboxylate pendants (**H_4L^1**; Chart 1), which forms stable complexes with Ln^{III} ions in an aqueous solution. In these complexes, the Ln^{III} ion is nine-coordinate, where a water molecule completes the inner coordination sphere. The relaxivity of this complex at the imaging fields (5.0 $s^{-1}\ mM^{-1}$ at 20 MHz and 25 °C) is comparable to those reported for the standard contrast agents (4.74 and 4.69 $s^{-1}\ mM^{-1}$ at 20 MHz and 25 °C for $[Gd(DOTA)(H_2O)]^-$ and $[Gd(DTPA)(H_2O)]^{2-}$, respectively). In the perspective of optimizing properties of Gd^{III} chelates as potential MRI contrast agents, herein we report two novel ligands (**H_6L^2** and **H_6L^3**; Chart 1) designed for stable complexation of Ln ions. A comparative study of the Ln complexes of these ligands allows for the assessment of how small structural modifications affect properties that are important with regard to MRI contrast agent applications, such as hydration number, water exchange rate, or rotational dynamics of the complexes. In particular, one can expect the introduction of the cyclohexyl unit in the ligand skeleton to modulate the rigidity of the inner sphere, which may have consequences on the water exchange for the Gd^{III} complexes. Luminescence lifetime studies on the Eu^{III} and Tb^{III} com-

(8) Peters, J. A.; Huskens, J.; Raber, D. *J. Prog. Magn. Reson. Spectrosc.* **1996**, *28*, 283.
(9) (a) Lukeš, I.; Cígler, P.; Kotek, J.; Rudovský, J.; Hermann, P.; Rohovec, J.; Vojtísek, P. *J. Inorg. Biochem.* **2001**, *86*, 68. (b) Kotek, J.; Lebdušková, P.; Hermann, P.; Vander Elst, L.; Muller, R. N.; Geraldes, C. F. G. C.; Maschmeyer, T.; Lukeš, I.; Peters, J. A. *Chem.—Eur. J.* **2003**, *9*, 5899.
(10) (a) Aime, S.; Botta, M.; Frullano, L.; Geninatti-Crich, S.; Giovenzana, G.; Pagliarin, R.; Palmisano, G.; Sirtori, F. R.; Sisti, M. *J. Med. Chem.* **2000**, *43*, 4017. (b) Aime, S.; Botta, M.; Geninatti-Crich, S.; Giovenzana, G.; Pagliarin, R.; Sisti, M.; Terreno, E. *Magn. Reson. Chem.* **1998**, *36*, S200.
(11) Aime, S.; Barge, A.; Borel, A.; Botta, M.; Chemerisov, S.; Merbach, A. E.; Müller, U.; Pubanz, D. *Inorg. Chem.* **1997**, *36*, 5104.
(12) (a) Ruloff, R.; Tóth, É.; Scopelliti, R.; Tripier, R.; Handel, H.; Merbach, A. E. *Chem. Commun.* **2002**, 2630. (b) Laus, S.; Ruloff, R.; Tóth, É.; Merbach, A. E. *Chem.—Eur. J.* **2003**, *9*, 3555.
(13) Powell, H. D.; Ni Dhubhghaill, O, M.; Pubanz, D.; Helm, L.; Lebedev, Y.; Schlaepfer, W.; Merbach, A. E. *J. Am. Chem. Soc.* **1996**, *118*, 9333.
(14) Cossy, C.; Helm, L.; Powell, D. H.; Merbach, A. E. *New J. Chem.* **1995**, *19*, 27.
(15) Mato-Iglesias, M.; Platas-Iglesias, C.; Djanashvili, K.; Peters, J. A.; Tóth, É.; Balogh, E.; Muller, R. N.; Vander Elst, L.; de Blas, A.; Rodríguez-Blas, T. *Chem. Commun.* **2005**, 4729.
(16) Platas-Iglesias, C.; Mato-Iglesias, M.; Djanashvili, K.; Muller, R. N.; Vander Elst, L.; Peters, J. A.; de Blas, A.; Rodríguez-Blas, T. *Chem.—Eur. J.* **2004**, *10*, 3579.

plexes have been carried out to determine the hydration number of the complexes in solution. To assess the hydration equilibrium, we have also performed a variable-temperature and -pressure UV−vis spectrophotometric study on the Eu^{III} complexes. Variable-temperature ^{17}O NMR measurements and nuclear magnetic relaxation dispersion (NMRD) investigation of the Gd^{III} complexes were carried out to obtain parameters describing rotation, electronic relaxation, and water exchange. Additionally, variable-pressure ^{17}O NMR measurements were used to determine the activation volume of the water exchange process and thus to assess the mechanism.

Experimental Section

Synthesis of the Ligands. Methyl 6-formylpyridine-2-carboxylate and 1,2-bis{[[6-(methoxycarbonyl)pyridin-2-yl]methyl]amino}-ethane (**2a**) were prepared as previously reported by us.[16] Solvents and starting materials were purchased from Aldrich and used without further purification, unless otherwise stated. Silica gel (Fluka 60, 0.063−0.2 mm) was used for preparative column chromatography.

(1*R*,2*R*)-{[[6-(Methoxycarbonyl)pyridin-2-yl]methylene]amino}-cyclohexane (1b). A solution of (1*R*,2*R*)-diaminocyclohexane (0.40 g, 3.5 mmol) in MeOH (10 mL) was added dropwise to a refluxing solution of methyl 6-formylpyridine-2-carboxylate (1.2 g, 7.0 mmol) in MeOH (30 mL). The resulting mixture was refluxed for 30 min and then filtered while hot. The solvent was removed in a rotary evaporator, and diethyl ether (10 mL) was added. The solid formed was isolated by filtration and dried under a vacuum to give 1.18 g of **1b** as a pale-yellow powder (yield: 83%). Anal. Calcd for $C_{22}H_{24}N_4O_4$: C, 64.7; H, 5.9; N, 13.7. Found: C, 64.2; H, 6.0; N, 13.9. FAB-MS [*m*/*z* (% BPI)]: 409 (100) [**1b** + H]$^+$. IR (KBr): 1737 [ν(C═O)], 1652 [ν(C═N)], 1586 [$\nu(C{=}N)_{py}$] cm^{-1}. ^{1}H NMR (solvent $CDCl_3$, 295 K, 300 MHz): δ 8.44 (s, 2H, −CH═N), 8.15 (d, 2H, py, ^3J = 7.7 Hz), 8.07 (d, 2H, py, ^3J = 7.7 Hz), 7.80 (t, 2H, py), 3.99 (m, 8H, $-OCH_3$, −CH−), 1.88 (m, 4H, $-CH_2-$), 1.79 (m, 2H, $-CH_2-$). ^{13}C NMR (solvent $CDCl_3$, 295 K, 75.5 MHz): δ 52.9 (primary C), 24.2, 32.6 (secondary C), 155.0, 137.4, 126.0, 124.3, 73.54 (tertiary C), 165.0, 160.7, 147.4 (quaternary C).

(1*R*,2*R*)-{[[6-(Methoxycarbonyl)pyridin-2-yl]methyl]amino}-cyclohexane (2b). $NaBH_4$ (0.07 g, 1.80 mmol) was added to a stirred suspension of **1b** (0.629 g, 1.50 mmol) in MeOH (60 mL) at 0 °C. The mixture was stirred at 0 °C for 2 h, and then a saturated $NaHCO_3$ aqueous solution (200 mL) was added. The mixture was stirred for 10 min, and the resulting solution was extracted with CH_2Cl_2 (5 × 100 mL). The combined organic extracts were dried over $MgSO_4$ and evaporated to give 0.583 g of **2b** as a pale-yellow oil, which was used in the next step without further purification (yield: 92%). FAB-MS [*m*/*z* (% BPI)]: 413 (100) [**2b** + H]$^+$. IR (Nujol): 1737 [ν(C═O)] cm^{-1}. ^{1}H NMR (solvent $CDCl_3$, 295 K, 300 MHz): δ 7.99 (d, 2H, py, ^3J = 7.6 Hz), 7.79 (t, 2H, py,), 7.71 (d, 2H, py, ^3J = 7.6 Hz), 4.17 (d, 2H, $-CH_2-$, ^2J = 14.8 Hz), 3.97 (d, 2H, $-CH_2-$, ^2J = 14.8 Hz), 3.96 (s, 6H, $-OCH_3$), 2.4−1.0 (m, 5H, cyclohexyl). ^{13}C NMR (solvent $CDCl_3$, 295 K, 75.5 MHz): δ 53.0 (primary C), 52.5, 31.9, 25.2 (secondary C), 137.6, 126.0, 123.6, 61.7 (tertiary C), 166.1, 161.8, 147.5 (quaternary C).

***N*,*N*′-Bis[(6-carboxy-2-pyridyl)methyl]ethane-1,2-diamine-*N*,*N*′-methylphosphonic Acid ($H_6L^2\cdot 2H_2O$). 2a** (1.40 g, 3.91 mmol) and an excess of phosphorous acid (2.50 g, 30.5 mmol) were dissolved in 20 mL of 6 M aqueous HCl. The resulting mixture was heated under an inert atmosphere (Ar) for 30 min, and paraformaldehyde (0.94 g, 30.5 mmol) was added in portions over a period of 48 h. After the addition of paraformaldehyde was complete, the reaction mixture was refluxed for 24 h. The resulting brown solution was concentrated under vacuum to obtain a brown oil, which was dissolved in 2 mL of 50% ethanol. After the solution was stirred for 24 h at room temperature, a white precipitate was formed, which was collected by filtration and dried under vacuum at 40 °C (yield: 0.89 g, 44%). Anal. Calcd for $C_{18}H_{24}N_4O_{10}P_2\cdot 2H_2O$: C, 39.0; H, 5.1; N, 10.1. Found: C, 38.8; H, 4.5; N, 10.1. IR (KBr): 1738 [ν(C═O)], 1597 [$\nu(C{=}N)_{py}$], 1358 [ν(P═O)] cm^{-1}. ^{1}H NMR (solvent D_2O, 295 K, 200 MHz, pD = 7.0): δ 7.69 (d, 4H, py), 7.34 (t, 2H, py), 4.07 (s, 4H, $-CH_2-$), 3.00 (s, 4H, $-CH_2-$), 2.81 (d, 4H, $-CH_2-$, $^2J_{HP}$ = 11 Hz). ^{13}C NMR (solvent D_2O, 295 K, 50.4 MHz, pD = 7.0): δ 52.1, 54.9, 60.4 (secondary C), 124.8, 127.3, 140.3 (tertiary C), 154.5, 173.8 (quaternary C). ^{31}P NMR (solvent D_2O, 25 °C, 81.1 MHz, pD = 7.0): δ 12.2.

***N*,*N*′-Bis[(6-carboxy-2-pyridyl)methyl]ethane-d_4-1,2-diamine-*N*,*N*′-methylphosphonic Acid (H_6L^2-d_4).** The preparation of ligand H_6L^2-d_4 (deuterated at the α position with respect to phosphonate groups) was carried out by a procedure similar to that described above for H_6L^2 by using compound **2a** (0.30 g, 0.84 mmol), phosphorous acid (0.55 g, 6.7 mmol), and deuterated paraformaldehyde (0.2 g, 6.7 mmol). The deuteration was confirmed by ^{1}H NMR spectroscopy (>95%).

***N*,*N*′-Bis[(6-carboxy-2-pyridyl)methyl]cyclohexane-(1*R*,2*R*)-diamine-*N*,*N*′-methylphosphonic Acid ($H_6L^3\cdot 4H_2O$).** Compound **2b** (1.2 g, 2.91 mmol) and an excess of phosphorous acid (1.90 g, 23.0 mmol) were dissolved in 30 mL of 6 M aqueous HCl. The resulting mixture was heated under an inert atmosphere (Ar) for 30 min, and paraformaldehyde (0.70 g, 23.0 mmol) was added in portions over a period of 6 h. After the addition of paraformaldehyde was complete, the reaction mixture was refluxed for 72 h. The resulting brown solution was concentrated under vacuum to obtain a brown oil, which was dissolved in methanol (2 mL). The addition of acetone causes the precipitation of a white solid, which was isolated by filtration and dried under vacuum at 40 °C (yield: 0.46 g, 38%). Anal. Calcd for $C_{19}H_{26}N_4O_{10}P_2\cdot 4H_2O$: C, 41.0; H, 5.9; N, 8.7. Found: C, 41.2; H, 5.4; N, 8.6. IR (KBr): 1737 [ν(C═O)], 1590 [$\nu(C{=}N)_{py}$], 1348 [ν(P═O)] cm^{-1}. ^{31}P NMR (solvent D_2O, 295 K, 125.8 MHz, pD = 7.0): δ 15.5, 9.4.

General Methods. Elemental analyses were carried out on a Carlo Erba 1108 elemental analyzer. FAB-MS spectra were recorded using a Fisons Quatro mass spectrometer with a Cs ion gun and 3-nitrobenzyl alcohol as the matrix. IR spectra were recorded, as KBr disks, using a Bruker Vector 22 spectrophotometer. High-resolution ^{1}H and ^{13}C NMR spectra were run at 25 °C with Bruker AC200 F or Bruker Avance 300-MHz spectrometers. Chemical shifts are reported as δ values. For measurements in D_2O, *tert*-butyl alcohol was used as an internal standard with the methyl signal calibrated at δ 1.2 (^{1}H) and 31.2 (^{13}C). ^{2}H NMR spectra (46.1 MHz) were recorded on a Varian INOVA-300 spectrometer. Longitudinal ^{2}H NMR relaxation times T_1 were measured by the inversion−recovery pulse sequence.[17]

Sample Preparation. The Ln^{III} complexes of L^2 and L^3 were prepared by mixing equimolar amounts of hydrated $LnCl_3$, $Ln(NO_3)_3$, or $Ln(ClO_4)_3$ (Ln = La, Eu, Gd, or Tb) and the ligand; pH values were adjusted with the aid of dilute solutions of NH_4OH (L^2) or NaOH (L^3) and HCl. The concentrations and pH values of the solutions used were as follows. $La^{III}L^2$-d_4: 10−137 mM, pH

(17) Vold, R. L.; Waugh, J. S.; Klein, M. P.; Phelps, D. E. *J. Chem. Phys.* **1968**, *48*, 3831.

7.05 (^{2}H NMR). $Eu^{III}\mathbf{L^2}$: 25 mM, pH 6.64 (UV−vis); 1.2 mM, pH 8.5 (luminescence). $Gd^{III}\mathbf{L^2}$: 4.87 mM, pH 6.94 (NMRD); 95.15 mmol·kg^{-1}, pH 7.09 (^{17}O NMR T_1 and T_2 measurements at 7.05 T), and 33.16 mmol·kg^{-1}, pH 9.20 (^{17}O NMR at 9.4 T). $Tb^{III}\mathbf{L^2}$: 1.6 mM, pH 8.5 (luminescence). $Eu^{III}\mathbf{L^3}$: 20 mM, pH 5.5 (UV−vis); 3.1 mM, pH 8.2 (luminescence). $Gd^{III}\mathbf{L^3}$: 20.05 mmol·kg^{-1}, pH 5.73 (^{17}O NMR); 1.0 mM, pH 6.55 (NMRD); $Tb^{III}\mathbf{L^3}$: 3.1 mM, pH 8.4 (luminescence).

Luminescence Measurements. Excitation and emission spectra were recorded on a Perkin-Elmer LS-50B spectrometer equipped for low-temperature (77 K) measurements. Luminescence lifetimes were calculated from the monoexponential fitting of the average decay data, and they are averages of at least three to five independent determinations.

UV−Vis Spectroscopy. UV−visible spectra on solutions of the Eu^{III} complexes of $\mathbf{L^2}$ and $\mathbf{L^3}$ were recorded in the temperature range 15.5−84.7 °C on a Perkin-Elmer Lambda 19 spectrometer, in thermostatizable cells with a 5-cm optical length (λ = 576.5−581.5 nm). For the variable-pressure measurements carried out at 333 K, a "Le Noble" piston-type cell was used.[18] The technique has been described in detail in a previous publication.[19]

^{17}O NMR Measurements. Variable-temperature ^{17}O NMR longitudinal (T_1) and transverse (T_2) relaxation time measurements on aqueous solutions of the Gd^{III} complexes were obtained on a Varian INOVA-300 spectrometer operating at 7.05 T, 40.7 MHz [for $Gd\mathbf{L^2}(H_2O)_q$] or on a Bruker ARX 400 spectrometer, 9.4 T, 54.2 MHz [for $Gd\mathbf{L^2}(H_2O)_q$ and $Gd\mathbf{L^3}(H_2O)_q$]. They were referenced to an acidified water solution (aqueous $HClO_4$, pH 3.3). Longitudinal ^{1}H and ^{17}O NMR relaxation times T_1 were measured by the inversion−recovery pulse sequence,[17] and the transverse relaxation times (T_2) were obtained by the Carr−Purcell−Meiboom−Gill spin−echo technique.[20] For the 9.4-T measurements, the samples were sealed in glass spheres that fitted into 10-mm NMR tubes, to eliminate susceptibility corrections to the chemical shifts.[21] For the 7.05-T measurements, the difference between the chemical shifts of proton signals of *tert*-butyl alcohol in the paramagnetic sample and in pure water was used to correct the ^{17}O NMR shift for the contribution of the bulk magnetic susceptibility.[22] The temperature was measured by a substitution technique.[23] To improve sensitivity in ^{17}O NMR, ^{17}O-enriched water (11.4% $H_2{}^{17}O$, Isotrade GmbH) was added to the solutions to yield around 1% ^{17}O enrichment. Variable-pressure ^{17}O NMR relaxation rates at 333 K were measured up to a pressure of 150 MPa on a Bruker ARX-400 spectrometer equipped with a homemade high-pressure probehead.[24]

NMRD. The $1/T_1$ NMRD profiles of the Gd^{III} complexes of $\mathbf{L^2}$ and $\mathbf{L^3}$ were recorded at 5, 25, and 37 °C with a Stelar field cycling system covering a range of magnetic fields from 2.3474×10^{-4} to 0.35 T (corresponding to a proton Larmor frequency range of 0.01−15 MHz) for $Gd\mathbf{L^2}(H_2O)_q$ and from 2.35×10^{-4} to 0.47 T (0.01−20 MHz) for $Gd\mathbf{L^3}(H_2O)_q$. Additional points were obtained on Bruker Minispec PC-20 (20 MHz), mq30 (30 MHz), mq40 (40 MHz), and mq60 (60 MHz) relaxometers, respectively.

Data Analysis. The analysis of ^{17}O NMR, NMRD, and UV−vis data was performed with a program working on a Matlab's platform version 6.5[25] or using a Micromath Scientist version 2.0 (Salt Lake City, UT). The reported errors correspond to 1 standard deviation obtained by statistical analysis.

Scheme 1[a]

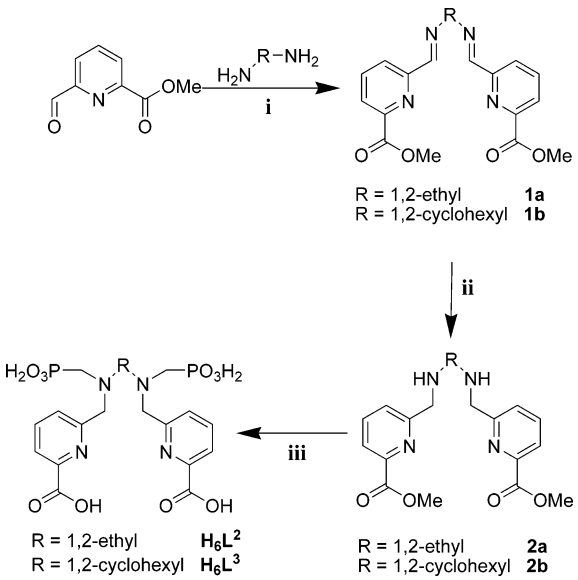

[a] (i) MeOH, reflux. (ii) MeOH, $NaBH_4$. (iii) 6 M HCl, CH_2O, H_3PO_3.

Results and Discussion

Synthesis of the Ligands. Ligands $\mathbf{H_6L^2}$ and $\mathbf{H_6L^3}$ were obtained in three steps from methyl 6-formylpyridine-2-carboxylate by using the procedure described in the Experimental Section (Scheme 1). The latter can be obtained from commercially available pyridine-2,6-dicarboxylic acid in three steps involving partial reduction of dimethyl pyridine-2,6-dicarboxylate followed by oxidation with SeO_2 (67% overall isolated yield).[16,26] Methyl 6-formylpyridine-2-carboxylate was reacted with ethane-1,2-diamine or (1*R*,2*R*)-diaminecyclohexane to give the Schiff bases **1a** and **1b** in 80−90% yield. Compounds **1a** and **1b** were reduced with sodium tetrahydroborate, affording amines **2a** and **2b** in excellent yield (ca. 90%). The desired ligands were prepared in 20−40% isolated yield by a Mannich-type reaction of the corresponding diamine precursor **2a** or **2b** with paraformaldehyde and phosphorous acid in 6 M HCl.[27] The ligands were obtained in ca. 20% overall yields as calculated from commercially available pyridine-2,6-dicarboxylic acid.

Assessment of the Hydration State. Luminescence lifetime measurements have been widely used for quantifying the number of inner-sphere water molecules in Ln complexes.[28] Although ions that emit in the near-IR such as Yb^{III} have been used for this purpose,[29] Tb^{III} and Eu^{III} are most commonly applied for lifetime measurements because they

(18) le Noble, W. J.; Schlott, R. *Rev. Sci. Instrum.* **1976**, *54*, 2540.
(19) Graeppi, N.; Powell, D. H.; Laurenczy, G.; Zékány, L.; Merbach, A. E. *Inorg. Chim. Acta* **1995**, *235*, 311.
(20) Meiboom, S.; Gill, D. *Rev. Sci. Instrum.* **1958**, *29*, 688.
(21) Hugi, A. D.; Helm, L.; Merbach, A. E. *Helv. Chim. Acta* **1985**, *68*, 508.
(22) Zitha-Bovens, E.; Vander Elst, L.; Muller, R. N.; van Bekkum, H.; Peters, J. A. *Eur. J. Inorg. Chem.* **2001**, 3101.
(23) Amman, C.; Meyer, P.; Merbach, A. E. *J. Magn. Reson.* **1982**, *46*, 319.
(24) Frey, U.; Helm, L.; Merbach, A. E. *High Press. Res.* **1990**, *2*, 237.
(25) Yerly, F. Visualiseur, version 2.3.4; Lausanne, Switzerland, 1999. Yerly, F. Optimiseur, version 2.3.4; Lausanne, Switzerland, 1999.
(26) Chrystal, E. J. T.; Couper, L.; Robins, D. J. *Tetrahedron* **1995**, *51*, 10241.
(27) Lázár, I.; Hrncir, D. C.; Kim, W.-D.; Kiefer, G. E.; Sherry, A. D. *Inorg. Chem.* **1992**, *31*, 4422.
(28) Horrocks, W. D., Jr.; Sudnick, D. R. *Acc. Chem. Res.* **1981**, *14*, 384.
(29) Dickins, R. S.; Aime, S.; Batsanov, A. S.; Beeby, A.; Botta, M.; Bruce, J. I.; Howard, J. A. K.; Love, C. S.; Parker, D.; Peacock, R. D.; Puschmann, H. *J. Am. Chem. Soc.* **2002**, *124*, 12697.

Table 1. Lifetimes of the Eu($^5D_0$) and Tb($^5D_4$) Excited Levels (τ, ms) and Number of Coordinated Water Molecules (q) Obtained in 10^{-3} M H_2O and D_2O Solutions of **L²** and **L³** Complexes (pH 8.0)[a]

	L²		**L³**	
	Eu^{III}	Tb^{III}	Eu^{III}	Tb^{III}
τ_{H_2O}	0.80	2.30	0.73	2.13
τ_{D_2O}	2.01	4.10	2.21	2.69
Δk_{obs}	0.75	0.19	0.91	0.13
q^b	0.6	0.7	0.8	0.4
q^c	0.5		0.7	

[a] The emission decay was monitored at 616 (Eu^{III}) or 490 (Tb^{III}) nm under excitation at 245 nm. [b] Values obtained by using eqs 1 (Eu^{III}) and 2 (Tb^{III}). [c] Values obtained by using eq 3.

emit in the visible region and show longer emission lifetimes. These two ions flank Gd^{III} in the periodic table, and therefore they have nearly the same charge-to-ionic radius as Gd^{III} and similar coordination chemistry. Therefore, the number of inner-sphere water molecules determined for Tb^{III} and Eu^{III} complexes should be close to the value for Gd^{III} complexes. Moreover, a desirable optical property of the Ln^{III} complexes of **L²** and **L³** is that the pyridine moieties can act as an antenna to sensitize the emission of Eu^{III} and Tb^{III}, which greatly increases the effective extinction coefficient of metal ion excitation and therefore improves the sensitivity of the luminescence detection.

The emission spectra of 10^{-3} M solutions of the Eu^{III} and Tb^{III} complexes of **L²** and **L³** in H_2O (pH 8.0 and 295 K), obtained under excitation through the ligand bands at 245 nm, display the typical $^5D_0 \rightarrow {}^7F_J$ (Eu^{III}, $J = 0-4$) or $^5D_4 \rightarrow {}^7F_J$ (Tb^{III}, $J = 6-3$) transitions. The emission lifetimes of the Eu($^5D_0$) and Tb($^5D_4$) excited levels have been measured in D_2O and H_2O solutions of the complexes and were used to calculate the number of coordinated water molecules q by using eqs 1 and 2 for Eu and Tb, respectively (Table 1). These equations were proposed by Beeby et al.[30] for solutions of poly(aminocarboxylate) complexes with $q \leq 1$,

$$q_{Eu} = 1.2(\Delta k_{obs} - 0.25) \quad (1)$$

$$q_{Tb} = 5.0(\Delta k_{obs} - 0.06) \quad (2)$$

where $k_{obs} = 1/\tau_{obs}$, $\Delta k_{obs} = k_{obs}(H_2O) - k_{obs}(D_2O)$, and k_{obs} is given in reciprocal milliseconds. More recently, a refined eq 3 has been proposed for Eu^{III} complexes in solution,[31] with an estimated uncertainty in q of ± 0.1.

$$q_{Eu} = 1.11(\Delta k_{obs} - 0.31) \quad (3)$$

The q values obtained for the Eu^{III} and Tb^{III} complexes of **L¹** and **L³** range from 0.5 to 0.8, suggesting that an equilibrium exists in solution between complex species with $q = 0$ and 1 (Table 1).

To learn more about the hydration state of the Ln^{III} complexes of **L²** and **L³**, we performed a variable-temperature and -pressure UV−vis study on aqueous solutions of the Eu^{III} analogues. The $^5D_0 \leftarrow {}^7F_0$ transition band of Eu^{III} (577.5−581.1 nm) is very sensitive to the coordination environment and is often used to test the presence of different complex species.[19,32] In the region of the $^5D_0 \leftarrow {}^7F_0$ transition, the spectrum of the Eu^{III} complex of **L²** shows two absorption bands at 578.9 and 579.4,[15] while that of **L³** shows signals at 579.0 and 579.6 nm (Figure 1). The intensity ratio of these bands changes with temperature: the band at shorter wavelengths is decreasing, while that at longer wavelengths is increasing with temperature. This temperature dependence can be explained in terms of a hydration equilibrium, where the band at lower energy is assigned to eight-coordinate, nonhydrated $[Eu(L)]^{3-}$, while that at ca. 579 nm is attributed to nine-coordinate, monohydrated $[Eu(L)(H_2O)]^{3-}$ (L = **L²**, **L³**):

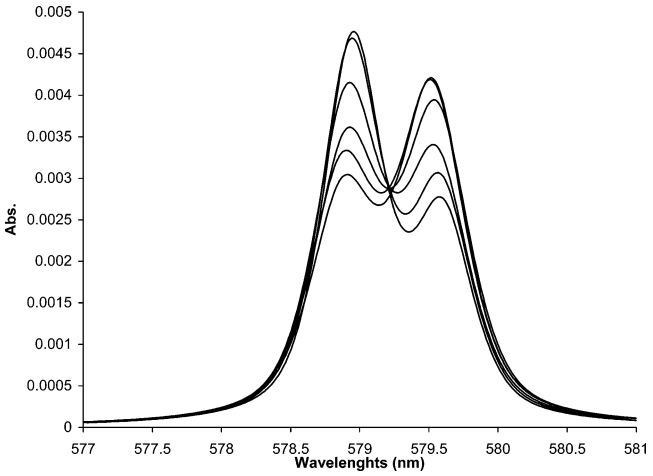

Figure 1. Variable-temperature UV−vis spectra of $[Eu(\mathbf{L^3})(H_2O)_q]^{3-}$ ($q = 0$, 1; $c = 20$ mM; pH 5.5).

$$[Eu(L)]^{3-} + H_2O \rightleftarrows [Eu(L)(H_2O)]^{3-} \quad (4)$$

Because the concentration of the solvent water is effectively constant, the equilibrium constant corresponding to eq 4 may be written as

$$K_{Eu} = \frac{[Eu(L)(H_2O)]}{[Eu(L)]} \quad (5)$$

The reaction enthalpy, ΔH^0, and the reaction entropy, ΔS^0, for the equilibrium may be obtained from the temperature dependence of K_{Eu}:

$$\ln K_{Eu} = \frac{\Delta S^0}{R} - \frac{\Delta H^0}{RT} \quad (6)$$

Similarly, the reaction volume can be obtained from the pressure dependence of K_{Eu}:

$$\ln K_{Eu} = \ln K_{Eu,0} - \frac{\Delta V^0 P}{RT} \quad (7)$$

where $K_{Eu,0}$ is the equilibrium constant at zero pressure. The temperature-dependent equilibrium constants for the hydra-

(30) Beeby, A.; Clarkson, I. M.; Dickins, R. S.; Faulkner, S.; Parker, D.; Royle, L.; de Sousa, A. S.; Williams, J. A. G.; Woods, M. *J. Chem. Soc., Perkin Trans. 2* **1999**, 493.
(31) Supkowski, R. M.; Horrocks, W. D., Jr. *Inorg. Chim. Acta* **2002**, *340*, 44.
(32) Platas-Iglesias, C.; Corsi, D. M.; Vander Elst, L.; Muller, R. N.; Imbert, D.; Bünzli, J.-C. G.; Tóth, É.; Maschmeyer, T.; Peters, J. A. *J. Chem. Soc., Dalton Trans.* **2003**, 727.

Table 2. Thermodynamic Parameters Determined by UV−Vis Spectrophotometry for the Hydration Equilibrium in Eq 4

ligand	K_{Eu}^{298}	$\Delta H^{0\,a}$	$\Delta S^{0\,b}$	$\Delta V^{0\,c}$
L²	1.8 ± 0.3	−11.6 ± 2	−34 ± 5	−4.1 ± 0.8
L³	1.7 ± 0.3	−13.5 ± 1	−41 ± 4	−6.7 ± 1.0

[a] Data in kJ·mol^{-1}. [b] Data in J·mol^{-1}·K^{-1}. [c] Data in cm^3·mol^{-1}; values determined at 333 K.

tion equilibrium (4) have been determined as previously described.[19] In this analysis, K_{Eu} is assessed by making the assumption that the two $^5D_0 \leftarrow {}^7F_0$ transitions observed have the same oscillator strength. This hypothesis has been confirmed for complexes $[Eu(PDTA)(H_2O)_2]^-$ and $[Eu(HDTA)(H_2O)_3]$, for which the equilibrium is strongly shifted toward the eight- and nine-coordinate species, respectively.[19] The temperature and pressure dependences (see the Supporting Information) of the absorption spectra were used to determine the reaction enthalpy, ΔH^0, the reaction entropy, ΔS^0, and the reaction volume (Table 2). The results compiled indicate that the Eu^{III} complexes of **L²** and **L³** present similar average hydration numbers, with $q_{ave} = 0.64$ and 0.63 for **L²** and **L³**, respectively, at 298 K. These values are in fairly good agreement with those obtained from luminescence measurements for the Eu^{3+} complexes (Table 1). This agreement confirms that it is indeed correct to analyze the UV−vis spectra by assuming similar oscillator strengths for the two $^5D_0 \leftarrow {}^7F_0$ transitions. The thermodynamic parameters reported in Table 2 indicate that q changes importantly with temperature from ca. 0.71 at 278 K to ca. 0.45 at 353 K.

The reaction volumes obtained from variable-pressure UV−vis measurements (Table 2) are smaller than those calculated for other europium(III) poly(aminocarboxylates). For instance, a reaction volume of −13.3 cm^3·mol^{-1} has been determined for the hydration equilibrium in EDTA-Eu^{III}, and a reaction volume of −7.5 cm^3·mol^{-1} has been reported for the DO3A-Eu^{III} system.[33] These results suggest that an important rearrangement of the Eu^{III} coordination sphere occurs on going from species $q = 0$ to 1. The rearrangement of the metal ion coordination environment appears to be more important for the complex of **L²** ($\Delta V = -4.1$ cm^3·mol^{-1}) than for the complex of **L³** ($\Delta V = -6.7$ cm^3·mol^{-1}), which might be attributed to the higher rigidity of **L³** as compared to **L²**.

^{17}O NMR and NMRD Measurements. Variable-temperature ^{17}O NMR at 7.05 T and ^{1}H NMRD measurements have been previously reported for Gd**L²**$(H_2O)_q$ in the preliminary paper,[15] which evidenced an unprecedentedly fast water exchange. Here we have performed a combined ^{17}O NMR and ^{1}H relaxometric study on Gd**L³**$(H_2O)_q$ in order to determine parameters describing water exchange and rotational dynamics. Moreover, to assess an eventual pH dependence of the water exchange for Gd**L²**$(H_2O)_q$, additional ^{17}O NMR measurements have been carried out on this complex at pH 9.2. In addition to the previous ^{17}O NMR study,[15] herein we also report chemical shift measurements that allowed us to determine the hyperfine ^{17}O coupling constant, $A/\hbar$, for Gd**L²**$(H_2O)_q$, which in the preliminary report was fixed to a usual value. In the case of fast water exchange, as for Gd**L²**$(H_2O)_q$, the calculated value of the water exchange rate is directly dependent on the scalar coupling constant, and therefore it is important to experimentally assess $A/\hbar$.

Because of their charge and important structure ordering effect, phosphonate groups have a tendency to induce a second hydration sphere around the metal complexes.[34] By remaining in the proximity of the paramagnetic Gd^{III} center for a nonnegligible time, these second-sphere water molecules may represent a significant contribution to the overall proton relaxivity. The second-sphere term also contributes to longitudinal ^{17}O NMR relaxation, which is influenced by dipolar and quadrupolar contributions, both related to τ_R.[35] The second-sphere water feels the rotation of the chelate, and consequently the T_1 values will be affected by the presence of second-sphere water molecules. In contrast to T_1, ^{17}O NMR T_2 relaxation is mainly governed by the scalar mechanism and therefore remains insensitive to τ_R and thus to the presence of a second hydration shell. In the analysis of ^{1}H and ^{17}O NMR relaxation data on Gd**L²**$(H_2O)_q$ reported in the preliminary paper,[15] second-sphere contributions have not been taken into account. Therefore, here we have reanalyzed the previously published ^{17}O NMR T_2 and NMRD data by introducing two modifications: (i) we fixed the hyperfine ^{17}O coupling constant to the value obtained in the high-pH ^{17}O NMR study and (ii) a second-sphere contribution was considered. The data for Gd**L³**$(H_2O)_q$ have been analyzed in the same manner, with the exception of the scalar coupling constant, which was not fixed during the fitting procedure.

For both Gd**L²**$(H_2O)_q$ and Gd**L³**$(H_2O)_q$, the ^{17}O NMR data were analyzed simultaneously with the ^{1}H NMR relaxation rates. The hydration state at each particular temperature has been calculated from the equilibrium constant as determined by UV−vis spectrophotometry for the Eu^{III} analogue. A second-sphere contribution was considered for both hydrated and nonhydrated species. The data have been fitted to the common Solomon−Bloembergen−Morgan theory relating the observed paramagnetic relaxation rates to microscopic parameters. Altogether, a very high number of parameters (21) are involved in the fit, with several of them being common to ^{17}O and ^{1}H NMR data. The number of second-sphere water molecules was fixed to three per complex, based on quantum mechanical calculations.[36] These calculations showed that three second-sphere water molecules are in close proximity of the Gd^{III} ion with a Gd−O distance of ca. 4.1 Å, whereas the others are relatively distant (Gd−O distances above 5.3 Å). The distances between O and H atoms of the first-sphere coordinated water and Gd were also fixed based on

(33) Tóth, É.; Ni Dhubhghaill, O. M.; Besson, G.; Helm, L.; Merbach, A. E. *Magn. Reson. Chem.* **1999**, *37*, 701.

(34) (a) Aime, S.; Gianolio, E.; Corpillo, D.; Cavallotti, C.; Palmisano, M.; Sisti, M.; Giovenzana, G. B.; Pagliarin, R. *Helv. Chim. Acta* **2003**, *86*, 615. (b) Botta, M. *Eur. J. Inorg. Chem.* **2000**, 399.

(35) Lebdušková, P.; Sour, A.; Helm, L.; Tóth, É.; Kotek, J.; Lukeš, I.; Merbach, A. E. *Dalton Trans.* **2006**, 3399.

(36) Mato-Iglesias, M.; Balogh, E.; Platas-Iglesias, C.; Tóth, É.; de Blas, A.; Rodríguez-Blas, T. Unpublished results.

Table 3. Parameters Obtained from the Simultaneous Analysis of ^{17}O NMR and NMRD Data

parameter	Gd**L**^{1}(H$_2$O)^a	Gd**L**^{2}(H$_2$O)$_q$	Gd**L**^{3}(H$_2$O)$_q$	GdDTPA(H$_2$O)^b	Gd(H$_2$O)$_8^{3+\,b}$
q^{298}	1	0.64	0.63	1	8
k_{ex}^{298} [10^6 s^{-1}]	5.0	700 ± 80 490 ± 90^c	149 ± 12	3.3	800
$\Delta H^{\ddagger}$ [kJ·mol^{-1}]	40.1	22 ± 2	32 ± 2	51.6	15.3
$\Delta S^{\ddagger}$ [J·mol^{-1}·K^{-1}]	+17.8	-3 ± 6	$+18.9 \pm 6$	+53.0	−23.1
$\Delta V^{\ddagger}$ [cm^3·mol^{-1}]		$+8.3 \pm 1.0^d$	$+8.7 \pm 1.0$	+12.5	−3.3
$A/\hbar$ [10^6 rad·s^{-1}]	−2.3	-3.5 ± 0.3^e	-3.5 ± 0.3	−3.8	−5.3
τ_{RO}^{298} [ps]	55^f	155 ± 10^g	145 ± 13^h	58^f	41
E_r [kJ·mol^{-1}]	17.9	27.1 ± 0.8	22.0 ± 0.6	17.3	15.0
τ_V^{298} [ps]	12.6	22 ± 2	18 ± 2	25	7.3
Δ^2 [10^{20} s^{-2}]	1.2	0.82 ± 0.09	0.95 ± 0.10	0.46	1.19

^{a} Reference 16. ^{b} Reference 13. ^{c} pH 9.2. ^{d} Reference 15. ^{e} Obtained from measurements at pH 9.2 and then fixed for the analysis at pH 7.09. ^{f} The high fitted values obtained for the quadrupolar coupling constant explain the low τ_{RO} values. ^{g} From ^{2}H NMR of La**L**^{2}. ^{h} $\tau_{RH}/\tau_{RO} = 0.70 \pm 0.05$.

these calculations to 2.54 and 3.1 Å, respectively. Four parameters describe the relaxation contribution of the second-sphere water. The exchange rate of the second-sphere water, $k_{ex,2nd}^{298}$, was fixed to 2×10^{10} s^{-1}, based on the simulations by Borel et al.,[37] while its activation energy ($\Delta H^{\ddagger}_{2nd}$) was set to 20 kJ·mol^{-1}. The distances of the second-sphere O and H from the Gd ion were fixed to 4.1 and 3.5 Å, respectively.

The activation energy of the correlation time for the modulation of the zero-field splitting, E_v, had to be fixed to a value of 1 kJ·mol^{-1}; otherwise, unrealistically low values were obtained. In the simultanous fit of the 7.05-T ^{17}O NMR and the NMRD data for Gd**L**^{2}(H$_2$O)$_q$, the value of the hyperfine coupling constant ($A/\hbar$) was fixed to -3.5×10^6 rad·s^{-1}, the value obtained for the same complex in the high-pH study at 9.4 T, where chemical shifts have also been measured. The empirical constant describing the outer-sphere contribution to the ^{17}O NMR chemical shift, C_{os}, was fixed to 0. The rotational dynamics of the complexes has been evaluated by using different rotational correlation times for the motion of the Gd inner-sphere water O and Gd inner-sphere water H vector (τ_{RH} and τ_{RO}), as observed by ^{17}O NMR and ^{1}H NMRD, respectively.[38] Geometrical calculations show that the ratio of these two rotational correlation times ($\tau_{RH}^{298}/\tau_{RO}^{298}$) has to lie between 0.65 and 1. The quadrupolar coupling constant, $\chi(1 + \eta^2/3)^{1/2}$, was fixed to 7.58 MHz, the value of pure water. The best least-squares fits were obtained using parameters listed in Table 3. The diffusion constant, D_{GdH}^{298}, and its activation energy, E_{DGdH}, were calculated to be $(24 \pm 2) \times 10^{-10}$ m^2·s^{-1} and 26 ± 2 kJ·mol^{-1} for Gd**L**^{2}(H$_2$O)$_q$ and $(24 \pm 2) \times 10^{-10}$ m^2·s^{-1} and 32 ± 2 kJ·mol^{-1} for Gd**L**^{3}(H$_2$O)$_q$, respectively. The experimental data and the fitted curves for Gd**L**^{3}(H$_2$O)$_q$ are presented in Figure 2, while for Gd**L**^{2}(H$_2$O)$_q$, they are shown in the Supporting Information. All equations used in the fitting procedure are also given in the Supporting Information.

The pressure dependence of the transverse ^{17}O NMR relaxation rates gives access to the volume of activation, $\Delta V^{\ddagger}$, a potent tool in assigning the mechanism.[39] Transverse ^{17}O NMR relaxation rates, $1/T_{2r}$, were measured at $B = 9.4$ T and $T = 333$ K for Gd**L**^{3}(H$_2$O)$_q$ [analogous data for Gd**L**^{2}-

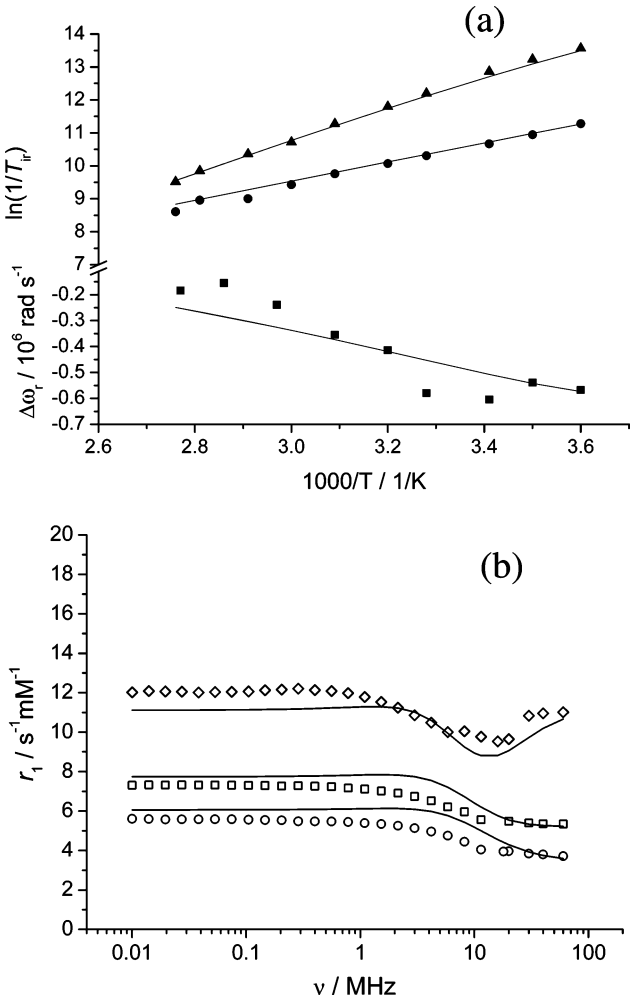

Figure 2. (a) Reduced longitudinal (●) and transverse (▲) ^{17}O NMR relaxation rates and ^{17}O chemical shifts (■) of a Gd**L**^{3}(H$_2$O)$_q$ solution at 9.4 T and pH 5.73. (b) ^{1}H NMRD profiles of a Gd**L**^{3}(H$_2$O)$_q$ at 5 (◇), 25 (□), and 37 °C (○) and pH 6.55. The reduced relaxation rates and chemical shifts in this figure are defined as $1/T_{1r} = [1/(c_{Gd}/55.5)][1/T_1 - 1/T_{1A}]$; $\Delta\omega_r = [1/(c_{Gd}/55.5)](\omega - \omega_A)$, where T_1 and T_{1A} are the paramagnetic and diamagnetic relaxation times, ω and ω_A are the paramagnetic and diamagnetic chemical shifts, and c_{Gd} is the concentration of the complex. The lines represent a simultaneous fit of ^{17}O NMR and NMRD data as explained in the text.

(37) Borel, A.; Helm, L.; Merbach, A. E. *Chem.—Eur. J.* **2001**, *7*, 600.
(38) Dunand, F. A.; Borel, A.; Merbach, A. E. *J. Am. Chem. Soc.* **2002**, *124*, 710.
(39) Lincoln, S. F.; Merbach, A. E. *Adv. Inorg. Chem.* **1995**, *42*, 1.

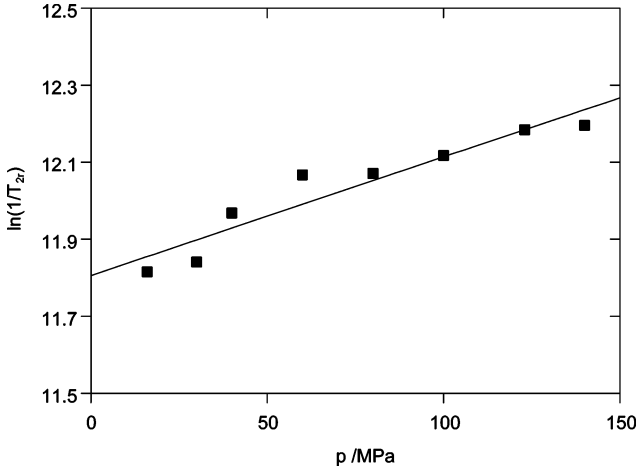

Figure 3. Variable-pressure reduced transverse ^{17}O relaxation rates measured in a Gd**L**^{3}$(H_2O)_q$ solution at 333 K and 9.4 T. Each $1/T_{2r}$ value has been calculated by taking into account the pressure dependence of the hydration equilibrium, as determined by UV−vis for the Eu^{III} analogue. The line represents a least-squares fit to the experimental data points as explained in the text.

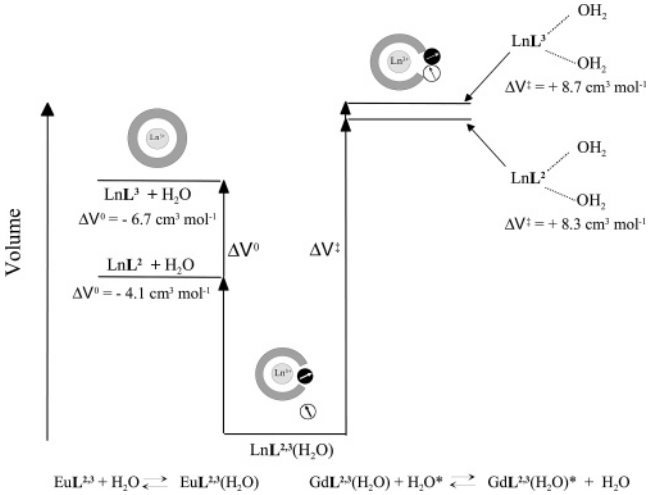

Figure 4. Volume profile showing the reaction volumes (from UV−vis measurements) for the hydration equilibrium observed in the Eu^{III} complexes of **L**^{2} and **L**^{4} and the activation volumes (from ^{17}O NMR data) for the water exchange reaction in the corresponding Gd^{III} chelates.

$(H_2O)_q$ were reported in the preliminary paper].[15] At the temperature and magnetic field used in the variable-pressure study, $1/T_{2r}$ is in the fast exchange limit and is dominated by the scalar interaction. For Gd**L**^{3}$(H_2O)_q$, the increase of $1/T_{2r}$ with pressure is, therefore, due to the slowing down of the water exchange process and suggests a dissociative interchange (I_d) mechanism. For each pressure, we calculated the individual hydration number on the basis of the pressure-dependent hydration equilibrium constant, as determined by the variable-pressure UV−vis study for the Eu^{III} analogue. The scalar coupling constant ($A/\hbar$) was previously found to be independent of pressure,[40] so we assumed that it is constant and equal to the value reported in Table 3. τ_v was also assumed to be pressure-independent. In fact, ascribing to τ_v a pressure dependence equivalent to activation volumes between -4 and $+4$ cm^3·mol^{-1} had a negligible effect on the fitted $\Delta V^{\ddagger}$ value. The experimental data points and results of the least-squares fits for Gd**L**^{3}$(H_2O)_q$ are shown in Figure 3. The fitted parameters are $\Delta V^{\ddagger} = (+8.7 \pm 0.8)$ cm^3·mol^{-1}, $(k_{ex})_0^{333} = (4.7 \pm 0.8) \times 10^8$ s^{-1}. (The error on $\Delta V^{\ddagger}$ is usually considered to be ± 1 cm^3·mol^{-1} or 10% of the $\Delta V^{\ddagger}$ value, whatever is the largest, to take into account possible effects of nonrandom errors.)

Water Exchange. The parameters characterizing water exchange are shown and compared to those of GdDTPA and $Gd(H_2O)_8^{3+}$ in Table 3. The rate of water exchange varies by 2 orders of magnitude between the acetate derivative Gd**L**^{1}(H_2O) and its phosphonate analogue Gd**L**^{2}$(H_2O)_q$, with an intermediate k_{ex}^{298} value for Gd**L**^{3}$(H_2O)_q$. Although k_{ex}^{298} calculated here for Gd**L**^{2}$(H_2O)_q$ by using an experimentally determined scalar coupling constant is slightly lower than what we have published in the preliminary paper,[15] it remains an extremely high value for a Gd^{III} chelate, being comparable to k_{ex}^{298} for the aqua ion. This very fast exchange is related to the presence of a hydration equilibrium for the chelate and, more importantly, to the very flexible inner coordination sphere around the metal ion. Other Gd^{III} complexes that also present hydration equilibrium do not necessarily have such extreme water exchange rates. For instance, GdDO3A and $GdDO2A^+$ both have differently hydrated species in aqueous solution ($q_{ave} = 1.8$ and 2.8, respectively), but they only show only a limited increase of the water exchange rate as compared to the monohydrated Gd(DOTA).[33] In addition to the decreased negative charge, which has a "slowing" effect in dissociatively activated mechanisms, the flexibility of the inner sphere of these macrocyclic complexes is the main factor responsible for the limited increase in k_{ex}^{298}. The inner-sphere structure is always less rigid for complexes of nonmacrocyclic ligands. The introduction of the cyclohexyl ring in the amine backbone in **L**^{3} rigidifies the structure and, as a consequence, slows down the water exchange by a factor of 5 on the Gd^{III} complex. It is interesting to note that the same rigidifying effect also has consequences on the formation kinetics of the Ln complexes, which has been found to be much slower for Cydta than for EDTA complexes.[41]

For both Gd**L**^{2}$(H_2O)_q$ and Gd**L**^{3}$(H_2O)_q$, the mechanism of the water exchange is dissociative interchange, as proven by the positive activation volumes. This is typical of nine-coordinate species, implying that the exchange proceeds via an eight-coordinate transition state. Figure 4 presents volume profiles showing, on the one hand, the reaction volumes determined for the hydration equilibrium on the Eu^{III} complexes of **L**^{2} and **L**^{3} (from UV−vis measurements) and, on the other hand, the activation volumes for the water exchange reaction in the corresponding Gd^{III} complexes (from ^{17}O NMR data). For the water exchange reaction, similar activation volumes have been determined on both Gd**L**^{2}$(H_2O)_q$ and Gd**L**^{3}$(H_2O)_q$. However, the reaction volume of the hydration equilibrium is clearly smaller for Eu**L**^{2}-$(H_2O)_q$ than for Eu**L**^{3}$(H_2O)_q$. The ΔV° value obtained for the complex of **L**^{2} is considerably smaller than those previously reported for other europium(III) poly(aminocarboxylates),[6] which confirms that an important rearrangement

(40) Cossy, C.; Helm, L.; Merbach, A. E. *Inorg. Chem.* **1989**, *28*, 2699.

(41) Szilagyi, E.; Brücher, E. *Dalton* **2000**, 2229.

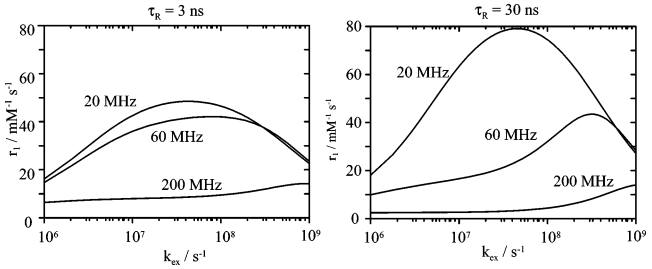

Figure 5. Calculated relaxivities as a function of the water exchange rate for various proton Larmor frequencies and rotational correlation times, τ_R. The simulations have been performed by using the common Solomon−Bloembergen−Morgan theory of paramagnetic relaxation.

of the Eu^{III} coordination sphere occurs on going from species $q = 0$ to 1. The inclusion of the cyclohexyl ring in the backbone in **L^3** rigidifies the structure of the chelate and, hence, limits the rearrangement of the metal coordination environment, which results in a larger ΔV^0 value for Eu**L^3**-$(H_2O)_q$ compared to Eu**L^2**$(H_2O)_q$.

In recent years, much interest has been devoted to the modulation of the water exchange rate on Gd^{III} complexes and, in particular, to the search for chelates with "optimal" water exchange for MRI contrast agent applications. Given the traditionally used MRI field strengths in clinics (20−60 MHz), the typical simulated curves of proton relaxivities as a function of the exchange rate have usually been performed for 20 MHz, and the values cited as "optimal" exchange rates varied around $(5-10) \times 10^7$ s^{-1}. Nowadays, higher and higher magnetic fields are entering clinical practice and experimental animal research in particular (400 MHz, 9.4 T or even higher).[42,43] The maximum relaxivities attainable at those high fields for Gd^{III}-based contrast agents are much lower than those at 20 MHz, which makes more important the optimization of the proton relaxation properties for Gd^{III} complexes. It is noteworthy to examine how the optimal value of the water exchange rate to attain the maximum relaxivity is varying with the magnetic field. Figure 5 shows calculated relaxivities as a function of the water exchange rate for three different frequencies and two rotational correlation times. It is clear from Figure 5 that the optimal water exchange rate shifts considerably to higher values with increasing magnetic field, and it also depends on the rotational correlation time. At high frequencies, extremely fast water exchange rates such as those found for Gd**L^2**$(H_2O)_q$ or Gd**L^3**$(H_2O)_q$ are needed to reach maximum relaxivities.

Rotation. The rotational correlation time, τ_R, is an important parameter to influence the proton relaxivity, and thus the efficiency of a MRI contrast agent. The relaxivities of both Gd**L^2**$(H_2O)_q$ and Gd**L^3**$(H_2O)_q$ (Figure 2) are typical of small-molecular-weight chelates. The value of the rotational correlation time, τ_R, can also be estimated from the deuterium longitudinal relaxation rate of the deuterated ligand complexed to the diamagnetic La^{III} ion.[44] To get information about the rotational correlation time of this family of Ln^{III} complexes in aqueous solutions, we prepared ligand **H$_6$L^2**-d_4, deuterated at the α position with respect to phosphonate groups. The synthesis of the deuterated ligand followed a procedure analogous to that used for the preparation of **H$_6$L^2**, with the exception of using deuterated paraformaldehyde. In diamagnetic systems, the longitudinal deuterium relaxation is fully controlled by quadrupolar interactions. Under the extreme narrowing condition ($\omega\tau_R \ll 1$), it is given by eq 8.

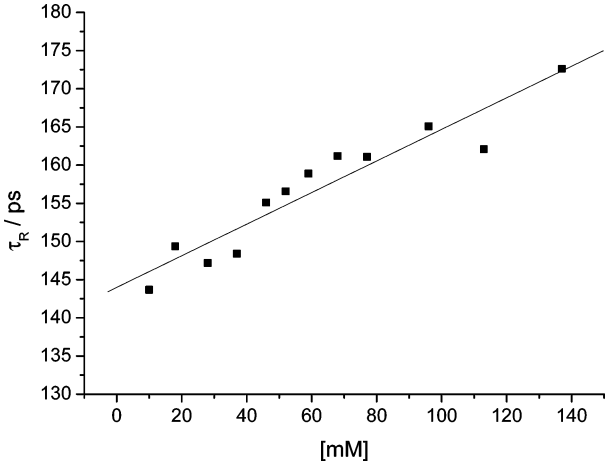

Figure 6. Rotational correlation times at 298 K (τ_R^{298}) obtained in water solutions of La(**L^2**-d_4)$(H_2O)_q$ at different concentrations.

$$R_1 = \frac{1}{T_1} = \frac{3}{8}\left(\frac{e^2qQ}{\hbar}\right)^2 \tau_R \qquad (8)$$

The quadrupolar coupling constant ($e^2qQ/\hbar$) depends on the degree of hybridization of the C−^{2}H bond and takes a value of approximately $170 \times 2\pi$ kHz for a C_{sp^3}−^{2}H bond.[45] The T_1 values for aqueous solutions of the La(**L^2**-d_4)$(H_2O)_q$ system increase upon dilution of the solution, while the calculated τ_R values decrease linearly (Figure 6). This effect was previously observed for different poly(aminocarboxylate) chelates,[32] and it has been attributed to a viscosity increase and to more important intermolecular interactions in concentrated solutions. The rotational correlation times obtained vary from 144 ps at a concentration of 10 mM to 172 ps at a concentration of 137 mM.

Conclusions

In this work, we have presented two new octadentate ligands designed for stable complexation of Ln ions. Lifetime measurements on solutions of the Eu^{III} and Tb^{III} complexes reveal the presence of a hydration equilibrium in solution between a nine-coordinate species containing one inner-sphere water molecule and an eight-coordinate species without any inner-sphere water molecules. This has been confirmed by a detailed analysis of the temperature and pressure dependence of the UV−vis spectra of the Eu^{III} complexes in the region where the $^5D_0 \leftarrow {}^7F_0$ transition occurs. The Gd^{III} complex of **L^2** presents an extremely fast water exchange rate of the inner-sphere water molecule, which it is attributed to the flexibility of the metal coordina-

(42) Pautler, R. G.; Fraser, S. E. *Curr. Opin. Immunol.* **2003**, *15*, 363 and references cited therein.
(43) Pautler, R. G. *Physiology* **2004**, *19*, 168.
(44) Vander Elst, L.; Laurent, S.; Muller, R. N. *Invest. Radiol.* **1998**, *33*, 828.
(45) Mantsch, H. H.; Saito, H.; Smith, I. C. P. *Prog. Nucl. Magn. Reson. Spectrosc.* **1977**, *11*, 211.

tion environment [$k_{ex}^{298} = (7.0 \pm 0.8) \times 10^8\ s^{-1}$]. Increasing the rigidity of the ligand by introducing a cyclohexyl moiety in the ligand backbone decreases the water exchange rate by a factor of 5 [$k_{ex}^{298} = (1.5 \pm 0.1) \times 10^8\ s^{-1}$ in Gd**L**^{3}$(H_2O)_q$]. Thus, on the basis of structural considerations, we were able to control the water exchange rate of the inner-sphere water molecule, an important parameter to be optimized in order to obtain new, more efficient MRI contrast agents.

Acknowledgment. We are grateful to Lothar Helm for scientific discussions. M.M.-I, C.P.-I., A.d.B., and T.R-B. thank Ministerio de Ciencia y Tecnología and FEDER (Grant BQU2001-0796), Xunta de Galicia (Grant PGIDIT02PXI10301PN), and Universidade da Coruña for financial support. É.T. and E.B. thank the Swiss National Science Foundation and the Swiss State Secretariat for Education and Research for financial support. This research was performed in the framework of the EU COST Action D18 "Lanthanide Chemistry for Diagnosis and Theraphy" and the European-founded EMIL program (Grant LSCH-2004-503569); their support and sponsorship are also kindly acknowledged.

Supporting Information Available: Equations used in the analysis of the ^{17}O NMR and NMRD data, variable-temperature transverse ^{17}O NMR relaxation rates and chemical shifts of Gd**L**^{2}-$(H_2O)_q$ at 9.4 T (pH 9.2) and parameters obtained from the fit of the experimental data, variable-temperature transverse and longitudinal ^{17}O NMR relaxation rates and chemical shifts and variable-pressure transverse ^{17}O NMR relaxation rates of Gd**L**^{3}$(H_2O)_q$ at 9.4 T, proton relaxivities of Gd**L**^{3}$(H_2O)_q$, Figures S1 and S2 showing the variation of ln K_{Eu} with temperature and pressure for Gd**L**^{3}$(H_2O)_q$, and Figures S3 and S4 showing reduced transverse and longitudinal ^{17}O NMR relaxation rates and chemical shifts of Gd**L**^{2}$(H_2O)_q$. This material is available free of charge via the Internet at http://pubs.acs.org.

IC0604157